Method of Moments Estimation for Energy Spectrum Sensing

Jesus Perez, Jesus Ibañez
Universidad de Cantabria
Santander, Spain
{jesus.perez, jesus.ibanez}@unican.es

***Abstract*—Energy detection is a well-known detection method for spectrum sensing in cognitive radio. Its low complexity and the fact that it does not require any prior knowledge of the primary signals, has made it a popular method. Despite its simplicity, energy detectors require knowing some parameters to set the decision threshold (according to a predefined criterion) and also to estimate its detection performance. Those parameters are the noise power, the primary signal power, and the duty cycle of the primary network. In this work, we propose a new sequential estimation method for jointly estimating those parameters from the energy measurements exclusively. Applying the Method of Moments, we derive the estimators as closed-form functions of the energy values. Their estimation performance is experimentally evaluated by means of over-the-air experiments with a testbed based on software-define-radio devices. The experiments also show the performance of the energy detectors with the estimated parameters.**

***Index Terms*—Spectrum sensing, energy detection, Method of Moments, experimental validation, software defined radio.**

I. Introduction

SPECTRUM sensing (SS) is a key operation in cognitive radio. Through SS the cognitive radios aim at detecting frequency bands that are not being used by the primary network. Energy detection is probably the most popular detection technique in SS [1]–[5] due to its simplicity and the fact that it does not require any prior knowledge of the signals to be detected. The energy detectors measure the energy received during a finite time interval, e, and compares it to a predetermined threshold, γ, to make a decision about the presence or absence of signals in the channel:

$$e \underset{\mathcal{H}_0}{\overset{\mathcal{H}_1}{\gtrless}} \gamma(\boldsymbol{\theta}), \tag{1}$$

where $\mathcal{H}_0$ and $\mathcal{H}_1$ refer to the null hypothesis and the alternative hypothesis, respectively.

A key aspect of energy detection is to set the threshold adequately. It depends on a set of parameters $\boldsymbol{\theta}$ which are unknown in practice, so they must be estimated. Moreover, they are needed to compute the detection performance. Those parameters are the noise power [6]–[9], the primary signal power at the energy detector [3], [5], [10], [11], and the channel occupancy rate (COR) also referred to as the duty cycle [12]–[17].

This work has been supported by the project ADELE PID2019-104958RB-C43, funded by MCIN/ AEI /10.13039/501100011033.

In this work, we assume the realistic scenario where the channel occupancy can dynamically change at random time while energy detection is in progress. This uncertainty makes parameter estimation a challenging problem. First, we consider a probabilistic mixture model of the energy measurements. Then, we apply the Method of Moments (MM) [18] to derive estimators for the three parameters with the following characteristics: 1) the parameters are estimated jointly and simultaneously from simple closed-form expressions of the energy measurements, 2) the estimators are fully blind, in the sense that they only depend on the energy measurements, and 3) the estimation is sequential. Each time a new energy measurement is available, the estimates are updated without the need to store previous energy measurements. The estimates $\hat{\boldsymbol{\theta}}$ can further serve to dynamically set the decision thresholds $\gamma(\hat{\boldsymbol{\theta}})$ and to estimate the detection performance at each time. To the best of our knowledge, no estimation method with the above characteristics has been proposed in the context of energy spectrum sensing.

The performance of the sequential MM-based detectors is experimentally evaluated by means of a testbed composed of Universal Software Radio Peripheral (USRP) devices [19]. First, we provide a detailed description of the testbed and the setup we have built for the over-the-air (OTA) experiments. Then, we show the performance of the MM estimators. The experiments also compare the MM-based detectors with the clairvoyant detector, that is, the one that employ the exact optimal decision threshold.

II. Energy measurements

Let $z(m)$ be the baseband complex signal received at the energy detector. It has to discriminate between the two hypotheses

$$\mathcal{H}_0 : z(m) = r(m), \qquad \mathcal{H}_1 : z(m) = y(m) + r(m),$$

where $y(m)$ is the primary user's signal and $r(m)$ is the noise. They are assumed to to be independent, zero-mean, white, complex circular Gaussian processes with variances σ_y^2 and σ_r^2, respectively. This is a standard assumption in the SS literature [20]–[22], which is particularly accurate when $y(m)$ is a multi-carrier modulated signal. The received signal samples, $z(m)$, will also be zero-mean, complex circular Gaussian distributed with variance $p = \sigma_r^2$ under $\mathcal{H}_0$, and $q = \sigma_r^2 + \sigma_y^2$ under $\mathcal{H}_1$.

Consequently, the primary signal-to-noise ratio (SNR) at the energy sensor is $(q-p)/p$.

The energy measurement from M signal samples is

$$e = \sum_{m=1}^{M} |z(m)|^2. \tag{2}$$

Assuming that the channel occupancy does not change during the samples acquisition, the energy measurements are distributed as scaled chi-squared random variables with $2M$ degrees of freedom:

$$\mathcal{H}_0 : e \sim \frac{p}{2}\ \chi^2_{2M}, \qquad \mathcal{H}_1 : e \sim \frac{q}{2}\ \chi^2_{2M}. \tag{3}$$

Then, the probabilities of false alarm and detection will be

$$P_{FA}(\boldsymbol{\theta}) = 1 - F_{\chi^2_{2M}}\left(\frac{2\gamma}{p}\right), \quad P_D(\boldsymbol{\theta}) = 1 - F_{\chi^2_{2M}}\left(\frac{2\gamma}{q}\right), \tag{4}$$

where $F_{\chi^2_{2M}}(\cdot)$ denotes the cumulative distribution function of χ^2_{2M}. Therefore, computing the P_{FA} and P_D of the energy detector requires knowing p and q, respectively. On the other hand, computing the probability of error also requires knowing the COR (prior probability of $\mathcal{H}_1$), which we will denote by u,

$$P_E(\boldsymbol{\theta}) = (1-u)\ P_{FA} + u\ P_D. \tag{5}$$

There are two main criteria for selecting the decision threshold, each related to one of the two fundamental approaches to the signal detection problem [2], [3]. They are the Neyman-Pearson (NP) criterion (also known as constant-false-alarm-rate criterion) and the minimum Bayes risk (MBR) criterion. The NP criterion aims to maximize the probability of detection subject to a constraint on the false alarm probability. The MBR criterion selects the threshold to minimize the so-called Bayesian risk (BR), which depends on predefined costs assigned to each type of error (false alarms and miss-detections). When the costs are identical, the BR reduces to the probability of error, and the MBR coincides with the maximum-a-posteriori (MAP) criterion.

Considering (4), the NP threshold for a prescribed probability of false alarm P^*_{FA} will be

$$\gamma_{NP}(\boldsymbol{\theta}) = \frac{p}{2}\ F^{-1}_{2M}(1 - P^*_{FA}). \tag{6}$$

which only depends on the noise power. The detector that minimizes the Bayes risk is [18]

$$\frac{f(e|\mathcal{H}_1)}{f(e|\mathcal{H}_0)} \underset{\mathcal{H}_0}{\overset{\mathcal{H}_1}{\gtrless}} \frac{C_{FA}}{C_D}\ \frac{1-u}{u}, \tag{7}$$

where $f(e|\mathcal{H}_i)$ denotes the probability density function (pdf) of the energy measurements under $\mathcal{H}_i$, and C_{FA} and C_{MD} are the costs assigned to the false alarms and miss-detections, respectively. Substituting the pdf of the energy measurements (3) into (7), and taking logarithms on both sides, the MBR detector can be written as follows

$$e \underset{\mathcal{H}_0}{\overset{\mathcal{H}_1}{\gtrless}} \frac{p\ q}{q-p} \log\left[\frac{q^M\ (1-u)\ C_{FA}}{p^M\ u\ C_{MD}}\right] = \gamma_{MBR}(\boldsymbol{\theta}). \tag{8}$$

Notice that the MRB threshold depends on p, q and u.

III. Method of Moments estimation

According to (3), the k-th order conditional moments of e are

$$\mathbb{E}[e^k|\mathcal{H}_0, p] = m_k\ p^k, \quad \mathbb{E}[e^k|\mathcal{H}_1, q] = m_k\ q^k, \tag{9}$$

where $m_k = \prod_{i=0}^{k-1}(M+i)$. Then, the k-th order marginal moment of the energy measurements is

$$\mathbb{E}[e^k|\boldsymbol{\theta}] = (1-u)\ \mathbb{E}[e^k|\mathcal{H}_0, p] + u\ \mathbb{E}[e^k|\mathcal{H}_1, q]. \tag{10}$$

Substituting (9) into (10) we get to,

$$\mu^{(k)} = (1-u)\ p^k + u\ q^k, \tag{11}$$

where $\mu^{(k)} = \frac{1}{m_k}\mathbb{E}[e^k|\boldsymbol{\theta}]$ is the scaled k-th order marginal moment. The equations for the first three moments in (11) constitutes the following system of nonlinear equations,

$$\begin{aligned} \mu^{(1)} &= (1-u)\ p + u\ q, \\ \mu^{(2)} &= (1-u)\ p^2 + u\ q^2, \\ \mu^{(3)} &= (1-u)\ p^3 + u\ q^3. \end{aligned} \tag{12}$$

From the first equation,

$$u = \frac{\mu^{(1)} - p}{q-p}. \tag{13}$$

Then, substituting (13) into the second and third equations, and after some simple algebraic manipulations, we obtain

$$\mu^{(2)} = (p+q)\mu^{(1)} - p\ q, \tag{14}$$

$$\mu^{(3)} = \left[(p+q)^2 - p\ q\right]\mu^{(1)} - p\ q(p+q). \tag{15}$$

Now, we consider the following change of variables,

$$\alpha = p + q, \tag{16}$$

$$\beta = p\ q, \tag{17}$$

so (14) and (15) can be written as

$$\mu^{(2)} = \alpha\ \mu^{(1)} - \beta \tag{18}$$

$$\mu^{(3)} = (\alpha^2 - \beta)\ \mu^{(1)} - \alpha\ \beta. \tag{19}$$

From (18),

$$\beta = \alpha\ \mu^{(1)} - \mu^{(2)}. \tag{20}$$

Substituting (20) into (19), the quadratic terms cancel and we obtain the following expression for α

$$\alpha = \frac{\mu^{(1)}\ \mu^{(2)} - \mu^{(3)}}{\mu^{(1)}\ \mu^{(1)} - \mu^{(2)}}. \tag{21}$$

Once α and β have been computed, p and q are obtained by reversing the change of variables. From (17), $p = \beta/q$. Then, substituting it into (16), we obtain

$$q = \frac{1}{2}\left(\alpha \pm \sqrt{\alpha^2 - 4\beta}\right). \tag{22}$$

Substituting (16) and (17) into (22) we find that the correct solution is the one associated to the plus sign. Finally, the estimate of the COR is computed from (13). In summary,

$$q = \frac{1}{2}\left(\alpha + \sqrt{\alpha^2 - 4\beta}\right), \qquad p = \frac{\beta}{q}, \qquad u = \frac{\mu^{(1)} - p}{q-p},$$

where α and β are given by (21) and (20), respectively.

A. Batch estimation

Let us consider a sequence of N consecutive energy sensing periods with energy measurements $\{e_1, \ldots, e_N\}$. We assume that the model parameters do not change during that time, but the channel occupancy can change between consecutive energy measurements. The scaled sample moments of the energy values are

$$\hat{\mu}_N^{(k)} = \frac{1}{m_k N} \sum_{n=1}^{N} e_n^k, \quad k = 1, 2, 3. \tag{23}$$

Then, replacing the moments $\mu^{(k)}$ by the sample moments (23), we obtain the MM estimators:

$$\hat{q}_N = \frac{1}{2}\left(\hat{\alpha}_N + \sqrt{\hat{\alpha}_N^2 - 4\hat{\beta}_N}\right), \; \hat{p}_N = \frac{\hat{\beta}_n}{\hat{q}_N}, \; \hat{u}_N = \frac{\hat{\mu}_N^{(1)} - \hat{p}_N}{\hat{q}_N - \hat{p}_N},$$

$$\hat{\alpha}_N = \frac{\hat{\mu}_N^{(1)}\,\hat{\mu}_N^{(2)} - \hat{\mu}_N^{(3)}}{\left(\hat{\mu}_N^{(1)}\right)^2 - \hat{\mu}_N^{(2)}}, \qquad \hat{\beta}_N = \alpha_N\,\hat{\mu}_N^{(1)} - \hat{\mu}_N^{(2)} \tag{24}$$

B. Sequential estimation

Since the energy values are measured sequentially, it is desirable to derive a sequential estimation method. When a new energy value, e_{n+1}, is measured, the scaled sample moments can be updated as

$$\hat{\mu}_{n+1}^{(k)} = \hat{\mu}_n^{(k)} + \eta_{n+1}\left[\frac{e_{n+1}^k}{m_k} - \hat{\mu}_n^{(k)}\right], \quad k = 1, 2, 3. \tag{25}$$

The initial values are $\hat{\mu}_0^{(k)} = 0$. The term $\eta_n \in (0, 1)$ is the learning rate (sometimes called forgetting factor) at time n. In stationary scenarios, where the model parameters do not change during the energy measurements, the learning rate is usually set to $\eta_n = n^{-1}$, so $\hat{\mu}_n^{(k)}$ coincides with the sample moments for the first n energy measurements. Consequently, the sequential estimates will coincide with the batch estimates. In non-stationary scenarios, where the parameters are time-varying, constant learning rates $\eta_n = \eta$ are typically used.

Note that estimates can be sequentially updated each time a new energy measurement is available, without the need to store previous energy measurements.

IV. Experimental evaluation

A. Testbed and experimental setup

We have considered a simple scenario where one node acts as a primary user (PU) and the other as the energy sensor. As nodes, we have used two B210 Universal Software Radio Peripheral (USRP) devices [19]. Both nodes used a single antenna with omnidirectional radiation pattern in the azimuth plane. The two nodes are connected to a personal computer (PC) via USB3.0 interfaces (see Figure 1). The PC is equipped with the GTEC Testbed Interface Software (GTIS) [23]. GTIS allows to easily configure and control the USRP nodes from the PC with MATLAB [24]. It also allows the PC to provide the transmitting node with the signal samples to be transmitted, and to store the samples acquired by the receiving node. The setup is shown in Figure 1. When the PU node is

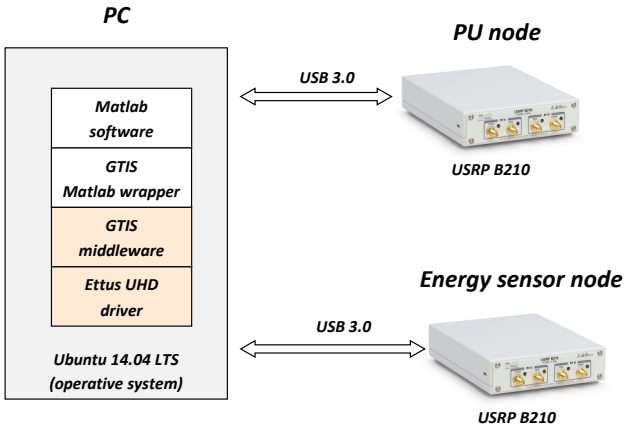

Fig. 1. Testbed and experimental setup.

active, it transmits OFDM 802.11a/g frames with 76 OFDM data symbols per frame using $64-$QAM modulation and $3/4$ coding rate. As a result, each frame has $L_f = 6000$ samples. The sampling rate is $f_s = 20$ Msamples per second, so the frame duration is $T_f = L_f \cdot f_s^{-1} = 0.3$ ms. The total channel bandwidth is 20 MHz with an occupied bandwidth of 16.6 MHz. The central frequency is 5.9 GHz.

We model the PU activity as a two states (active and inactive) homogeneous Markov chain with time steps equal to the frame duration T_f. In each frame interval, the PU transmits one frame if it is active, and remains silent if it is inactive. Markov models have been widely used to model the PU network activity in cognitive radio systems [25], [26]. In particular, we adopt the model in [26] where the transition probabilities $\mathrm{P}(\text{inactive} \to \text{inactive}) = 1 - u$, $\mathrm{P}(\text{active} \to \text{active}) = u$. Then, the average busy period duration is $T_f \cdot u/(1-u)$, and the average idle period duration is $T_f \cdot (1-u)/u$. Notice that other parameters (e.g. frames, PU activity model) could have been used for the experiments, since the MM estimators do not assume any. The sensing node

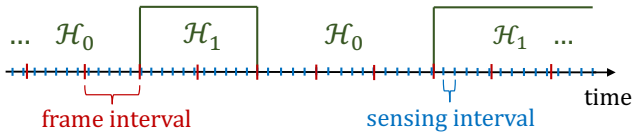

Fig. 2. PU activity pattern.

acquires samples, also at $f_s = 20$ Msamples/s to compute the energy values, e_n, by selecting the corresponding sets of M consecutive samples (2). The energy sensing interval (time elapsed between consecutive energy measurements) was $T_e = 60\mu$s, then, the average number of energy measurements per frame interval was 5. The sensing node is not synchronized with the PU node, so there could be energy measurements with some of the samples acquired when the PU is active and others when it is inactive. Although our energy model (3) does not consider these situations, they can occur in our experiments and in practical cases, especially when M is large.

Each experiment comprises $N = 400$ energy measurements, so it lasts $N \cdot T_e = 24$ ms. After each energy measurement, e_n, we sequentially update the estimates $\hat{\boldsymbol{\theta}}_n$, compute the decision threshold $\gamma(\hat{\boldsymbol{\theta}}_n)$ according to the selected criterion, apply the energy detector to e_n, and check whether the decision is correct or not. We average the results of $R = 320$ consecutive experiments under the same conditions.

In the initial energy sensing periods, when all energy values come from the same channel occupancy, the mixture model (10) is inappropriate. In those cases, the estimates (24) usually take invalid values. In particular, the term inside the square root in $\hat{q}_n$ can result negative and $\hat{u}_n$ out of range. When this happens we assume that the energy values have been measured under $\mathcal{H}_0$, so $\hat{u}_n = 0$, and $\hat{p}_n = \hat{q}_n = \mu_n^{(1)}$.

The experiments were conducted in the laboratory of the Signal Processing Group at the University of Cantabria in a rather static indoor environment. Each set of R experiments took about 8 seconds (there is some latency between consecutive experiments). We avoided anybody moving in the propagation environment to guarantee that q does not change during that time. Since, the model parameters $\boldsymbol{\theta}$ remained invariant during the experiments, we always used $\eta_n = n^{-1}$ as learning rate in (25).

To analyze the estimation and detection performance we must know the true values of p and q. Since they are unknown, we approximated them by the sample variances of all signal samples $z(m)$ acquired under $\mathcal{H}_0$ and $\mathcal{H}_1$, respectively, along the R experiments. The number of samples in each set of experiments was $Lf \cdot N_f \cdot R = 1.5 \cdot 10^8$, which guarantees that the sample variances are close to the true values of p and q. We call clairvoyant detector [18] the one that uses those values to set the decision threshold. Its performance can be considered as an upper bound for the MM-based detector.

B. Experimental results

Figures 3 and 4 show how the experimental bias and the root mean-squared-error (RMSE) of the estimates evolve with the number of energy measurements (n). The results correspond to the case $u = 0.3$, $M = 200$, and SNR = -8.13 dB. The bias and the RMSE of $\hat{p}_n$ and $\hat{q}_n$ are normalized.

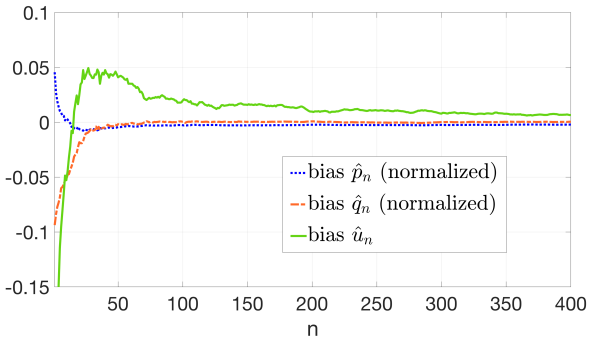

Fig. 3. Transient bias of the estimates.

Figure 5 compares the transient performance of the MM-based detector and the clairvoyant detector for two criteria: NP with $P_{FA}^* = 0.1$, and MBR with $C_{MD} = 5, C_{FA} = 1$. The conditions was as in previous figures 3 and 4.

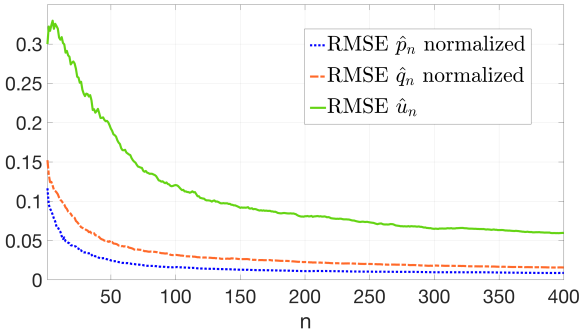

Fig. 4. Transient RMSE of the estimates.

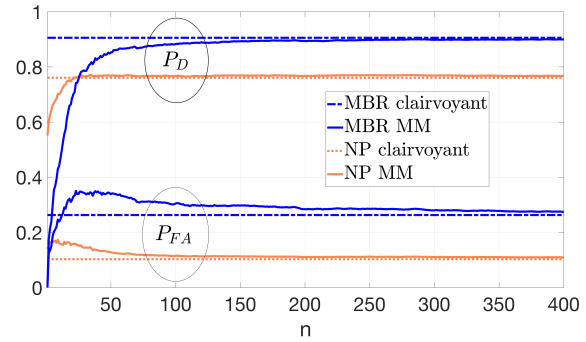

Fig. 5. Performance for the NP and MBR criteria with $P_{FA}^* = 0.1$ and $C_{MD} = 5, C_{FA} = 1$, respectively.

Figure 6 shows the detection performance of the MBR detectior, with $C_{MD} = 5, C_{FA} = 1$, for different values of M. The rest of the conditions was as in previous figures.

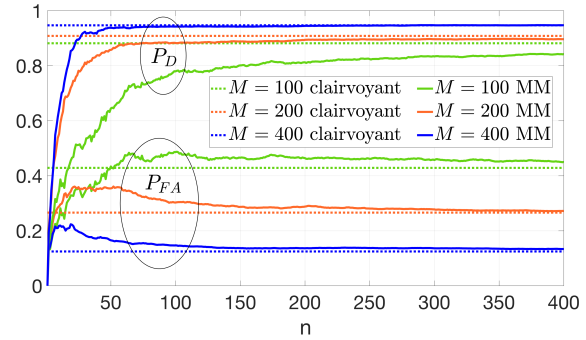

Fig. 6. Performance for the MBR criterion, with $C_{MD} = 5, C_{FA} = 1$, and different values of M.

Finally, 7 shows the probability of error for the MAP criterion and two different values of SNR. In this case $M = 400$ and $u = 0.3$.

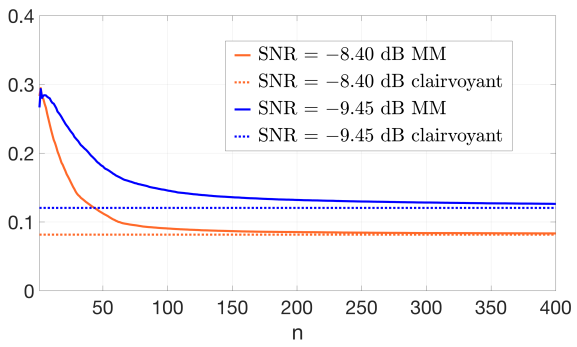

Fig. 7. Probability of error for the MAP criterion ($C_{MD} = C_{FA} = 1$), and different values of SNR.

V. CONCLUSIONS

We have presented a new blind sequential algorithm, based on the Method of Moments, for jointly estimate the parameters involved in energy detection. The parameter estimates are used to set the decision threshold and predict the detection performance. The algorithm has been experimentally evaluated by means of a testbed composed of software-define-radio devices. The experiments show that the algorithm can efficiently estimates the parameters, so the detection performance is close to the clairvoyant detector in realistic conditions.

REFERENCES

[1] H. Urkowitz, "Energy detection of unknown deterministic signals," *Proc. IEEE*, vol. 55, pp. 523–531, April 1967.

[2] H. V. Poor, *An introduction to signal detection and estimation*, Springer-Verlag, 1994.

[3] E. Axel, G. Leus, E.G. Larsson, and H.V. Poor, "Spectrum sensing for cognitive radio: state-of-art ad recent advances," *IEEE Signal Processing Magazine*, vol. 29, no. 3, pp. 101–116, May 2012.

[4] Y. Zeng, Y. C. Liang, A. T. Hoang Liu, and R. Zhang, "A review on spectrum sensing for cognitive radio: challenges and solutions," *EURASIP Journal on Advances in Signal Processing*, vol. 2010, no. 1, January 2010.

[5] Jesus Perez, Javier Via, Luis Vielva, and David Ramírez, "Online detection and snr estimation in cooperative spectrum sensing," *IEEE Transactions on Wireless Communications*, vol. 21, no. 4, pp. 2521–2533, 2022.

[6] R. Tandra and A. Sahai, "Snr walls for signal detection," *IEEE Journal of Selected Topics in Signal Processing*, vol. 2, pp. 4–17, February 2008.

[7] Andrea Mariani, Andrea Giorgetti, and Marco Chiani, "Effects of noise power estimation on energy detection for cognitive radio applications," *IEEE Transactions on Communications*, vol. 59, no. 12, pp. 3410–3420, 2011.

[8] P. B. Gohain, S. Chaudhari, and V. Koivunen, "Cooperative energy detection with heterogeneous sensors under noise uncertainty: Snr wall and use of evidence theory," *IEEE Transactions on Cognitive Communications and Networking*, vol. 4, no. 3, pp. 473–485, September 2018.

[9] Samar M. Hassan, Ashraf Eltholth, and Abdel Hady Ammar, "Double threshold weighted energy detection for asynchronous pu activities in the presence of noise uncertainty," *IEEE Access*, vol. 8, pp. 177682–177692, 2020.

[10] M. Lopez-Benitez and J. Lehtomaki, "Energy detection based estimation of primary channel occupancy rate in cognitive radio," in *IEEE Wireless Communications Network Conference - International Workshop on Smart spectrum (IWSS 2016)*, Doha, Qatar, April 2016, pp. 306–311.

[11] Jakub Nikonowicz, Aamir Mahmood, and Mikael Gidlund, "A blind signal samples detection algorithm for accurate primary user traffic estimation," *Sensors*, vol. 20, no. 15, 2020.

[12] A. Al-Tahmeesschi, M. Lopez-Benitez, V. Selis, D. K. Patel, and K. Umebayashi, "Cooperative estimation of primary traffic under imperfect spectrum sensing and byzantine attacks," *IEEE Access*, vol. 6, pp. 61651–61664, October 2018.

[13] J. Lehtomaki, R. Vuohtoniemi, and K. Umebayashi, "On the measurement of duty cycle and channel occupancy rate," *IEEE Journal on Selected Areas on Communications*, vol. 31, no. 11, pp. 2555–2565, November 2013.

[14] W. Gabran, C. H. Liu, P. Pawelczak, and D. Cabric, "Primary user traffic estimation for dynamic spectrum access," *IEEE Journal of Selected Areas on Communications*, vol. 31, no. 3, pp. 544–558, March 2013.

[15] J. Lehtomaki, M. Lopez-Benitez, K. Umebayashi, and M. Juntti, "Improved channel occupancy rate estimation," *IEEE Transactions on Communications*, vol. 63, no. 3, pp. 643–654, March 2015.

[16] M. Lopez-Benitez, A. Al-Tahmeesschi, D. K. Patel, and J. Lehtomaki, "Estimation of primary channel activity statistics in cognitive radio based on periodic spectrum sensing observations," *IEEE Transactions on Wireless Communications*, vol. 18, no. 2, pp. 983–996, February 2019.

[17] O. H. Toma, M. Lopez-Benitez, D. K. Patel, and K. Umebayashi, "Estimation of primary channel activity statistics in cognitive radio based on imperfect spectrum sensing," *IEEE Transactions on Communications*, vol. 68, no. 4, pp. 2016–2031, April 2020.

[18] S. M. Kay, *Fundamentals of Statistical Signal Processing. Detection Theory*, Prentice Hall. Signal Processing Series, 1998.

[19] Ettus Research LLC. Universal Software Radio, ," [online] http://www.ettus.com/, 2012.

[20] J. Ma, G. Zhao, and Y. Li, "Soft combination and detection for cooperative spectrum sensing in cognitive radio networks," *IEEE Transactions on Wireless Communications*, vol. 7, no. 11, pp. 4502–4507, December 2008.

[21] Z. Quan, S. Cui, and A. H. Sayed, "Optimal linear cooperation for spectrum sensing in cognitive radio networks," *IEEE Journal of Selected Topics in Signal Processing*, vol. 2, no. 1, pp. 28–40, February 2008.

[22] K. M. Thilina, K. W. Choi, N. Saquib, and E. Hossain, "Machine learning techniques for cooperative spectrum sensing in cognitive radio networks," *IEEE Journal on Selected Areas in Communications*, vol. 11, no. 10, pp. 2209–2221, November 2013.

[23] GTEC testbed project, ," [online] https://bitbucket.org/tomas_bolano/gtec_testbed_public.git., 2015.

[24] MATLAB, *version 9.1.0 (R2016b)*, The MathWorks Inc., Natick, Massachusetts, 2016.

[25] M. Wellens, J. Riihijärvi, and P. Mähönen, "Empirical time and frequency domain models of spectrum use," *Physical Communication*, vol. 2, no. 1, pp. 10–32, March 2009.

[26] M. Lopez-Benitez, *Spectrum usage models for the analysis, design and simulation of cognitive radio networks*, Ph.D. thesis, Universitat Politecnica de Catalunya, 2001.